


SHORT REPORT

Open Access



Development of non-destructive isotope measurement of the natural galena (PbS) using negative muon beams

K. Terada^{1,2*} , K. Ninomiya^{1,2}, A. Sato^{1,2}, D. Tomono^{2,3}, Y. Kawashima³, M. Inagaki¹, A. Nambu¹, T. Kudo¹, T. Osawa⁴ and M. K. Kubo⁵

Abstract

In Earth and planetary science, Pb isotopic composition is well known to play a key role in deciphering the origin and evolution of materials because they provide unique chronological and/or indigenous regional information as a radiogenic daughter nuclide from U and Th. To determine such an isotopic composition, mass spectrometers have been widely used over several decades, which requires a destructive/consuming treatment such as sputtering, laser ablation and thermal ionization. Here, we first report the non-destructive Pb isotopic measurement of natural galena (PbS) using the energy shift of muon-induced characteristic X-rays. The observed Pb isotopic composition of the natural galena is in good agreement with that obtained by conventional mass spectrometry. Such a muon-based Pb isotopic analysis method is expected to be applied to identify the production area of archaeological artefacts (e.g. bronze products), where non-destructive analysis is highly desirable compared to conventional mass spectrometry.

Keywords Isotope measurement, Muon analysis, Non-destructive analysis, Galena (PbS), Lead isotopes

Introduction

The isotopic compositions of a natural sample can provide useful information on the origin and/or physico-chemical processes such as evaporation, condensation, diffusion, isotopic exchange and radiometric decay. To determine such an isotopic composition, a mass

spectrometers have been widely used over several decades, which requires a destructive/consuming treatment such as sputtering, laser ablation and thermal ionization. Since the highly intense muon beam can be produced (Miyake et al 2009), muon-induced characteristic X-ray analysis has attracted interest because this brand-new analytical method has significant potential to determine the isotope ratios without any destruction, which is desirable for rare and precious samples such as planetary samples and/or archaeological artefacts.

The muon is one of the charged leptons with a mass of 105.7 MeV/c², approximately 200 times heavier than the electron. In the classical Bohr model, orbital radii of negative leptons (electron and/or muon) around an atomic nucleus are inversely proportional to the lepton mass. Because the energy gaps between orbits are also proportional to the lepton mass, cascade transitions of the trapped muon from higher- to lower-energy states emit the muonic characteristic X-ray with c.a. 200 times

*Correspondence:

K. Terada
terada@ess.sci.osaka-u.ac.jp

¹ Graduate School of Science, Osaka University, Toyonaka 560-0043, Japan

² Forefront Research Center, Osaka University, Toyonaka 560-0043, Japan

³ Research Center for Nuclear Physics, Osaka University, Ibaraki 567-0047, Japan

⁴ Materials Sciences Research Center, Japan Atomic Energy Agency (JAEA), Tokai 319-1195, Japan

⁵ College of Liberal Arts, International Christian University, Mitaka 181-8585, Japan

higher energy than that associated with the orbital transition of electrons. (For instance, electron-induced $K\alpha$ -X-rays of C and O have energies of 0.3, 0.5 keV, respectively, whereas muonic $K\alpha$ -X-rays of C and O have energies of 75, 134 keV, respectively.) We have successfully applied this sophisticated non-destructive elemental analysis to various meteorites and the returned sample from C-type asteroid Ryugu (Terada et al. 2014, 2017; Osawa et al. 2015, 2022; Nakamura et al. 2022, Chiu et al. 2023; Ninomiya et al. 2024).

Interestingly, the innermost orbit of the muon (the 1 s orbit) is extremely close to the nucleus and tends to be affected by the distribution of the nuclear charge. Therefore, the energy of characteristic X-ray changes depending on the mass of nuclides, which is called “isotope shift”. So far, energy shifts of some enriched isotope metals have been confirmed: Zn (Jenkins et al. 1970), Sn & Nd (Macagno et al. 1970), Ba (Kunold et al. 1983), Mo (Schellenberg et al. 1984), Ba (Kunold et al. 1983), Te (Shera et al. 1989), Sm (Strasser et al. 2009) and so forth. Recently, our research team also successfully demonstrated that the energy shifts of “normal” Pb metal (Ninomiya et al. 2019) and “normal” Ag metal (Osawa et al. 2020) can be detected using the pulsed muon beam at J-PARC (the Japan Proton Accelerator Complex (J-PARC)). It is well known that the Pb isotopic ratios are very informative not only for chronology in Earth and planetary science but also for identification of the production area of archaeological artefacts in archaeology. As a next step, we have applied this sophisticated method to natural terrestrial samples, specifically to galena (PbS) to determine the Pb isotope ratios non-destructively using a direct current (DC) muon beam (Fig. 1).

Method and experiment

The MUon Science Innovative Channel (MuSIC) facility at Research Center for Nuclear Physics (RCNP), Osaka University, Japan, was designed to produce a direct current (DC) muon beam with an extremely high proton-to-muon yield (10^8 muons/s with a 0.4 kW proton beam, 392 MeV proton energy with a current of 1 μ A (Fig. 2a). In order to produce an intense muon beam from the 0.4 kW proton beam, a novel pion capture system has been employed (Hino et al. 2014). A continuous proton beam extracted by a cyclotron accelerator bombards a cylindrical graphite target (4 cm in diameter and 20 cm in length) to produce pions that decay into muons and two neutrinos with a very short lifetime (26 ns). The momentum peak of the MuSIC muon beam at the current setting is ~ 70 MeV/c with a beam size of 5 cm. Since the first light of a muon beam in

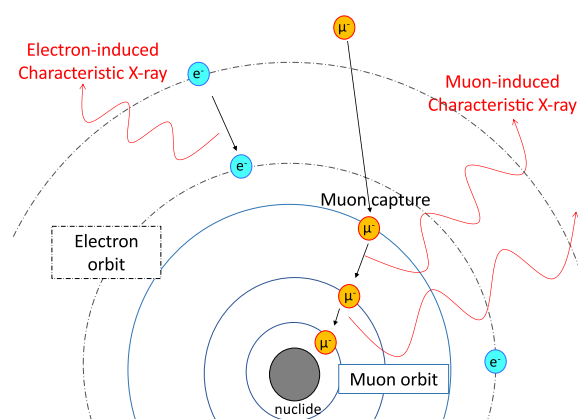


Fig. 1 Schematic view of the principle of muon-induced characteristic X-ray

2014, MuSIC has provided an intense DC muon beam with a momentum range of 20–120 MeV/c (Kohno 2015; Cook et al. 2017), which can also be applicable for non-destructive elemental analysis (Terada et al. 2017).

In this study, we conducted a muonic X-ray measurement of two samples: an enriched ^{208}Pb sample ($\Phi 30$ mm \times 0.35 mm: Pb ingot from ISOFLEX USA, ^{208}Pb : 99.57%, ^{207}Pb : 0.35%, ^{206}Pb : 0.01% and ^{204}Pb : 0.07%) and natural galena (PbS) from the Osarizawa mine, Japan (15 mm \times 25 mm \times 13 mm: ^{208}Pb : 52.8%, ^{207}Pb : 20.9%, ^{206}Pb : 24.9% and ^{204}Pb : 1.4% determined by LA-ICP mass spectrometry). The samples were placed in the centre of the muon beamline, 135 mm from the beamline exit. For X-ray detection, two high-purity germanium detectors were used for X-ray detection. One is the GC6020 (CANBERRA) with a diameter of 51.8 mm, and another is the BE3830 (CANBERRA) with a diameter of 30 mm.

Figure 2b, c illustrates the geometry of the analytical setting. Two Ge detectors were oriented at 90 degrees to the muon beam and GC6020 and BE3830 were placed at distance of 90 mm and 80 mm from the sample, respectively. A pair of plastic scintillators with the size of 30 mm \times 30 mm that detect the muon passage was also placed in front of the sample to trigger the X-ray counting system. By counting X-ray signals coincident with the signal from the plastic scintillators, we were able to reduce the signal-to-noise ratio dramatically. More details of the analytical setting are written in Ninomiya et al. (2022).

The muon flux on the sample was estimated as 500 muons/s by the counting rate of the plastic scintillation counters. The muon momentum was set to 60 MeV/c to obtain enough muon intensity. The exposure times to

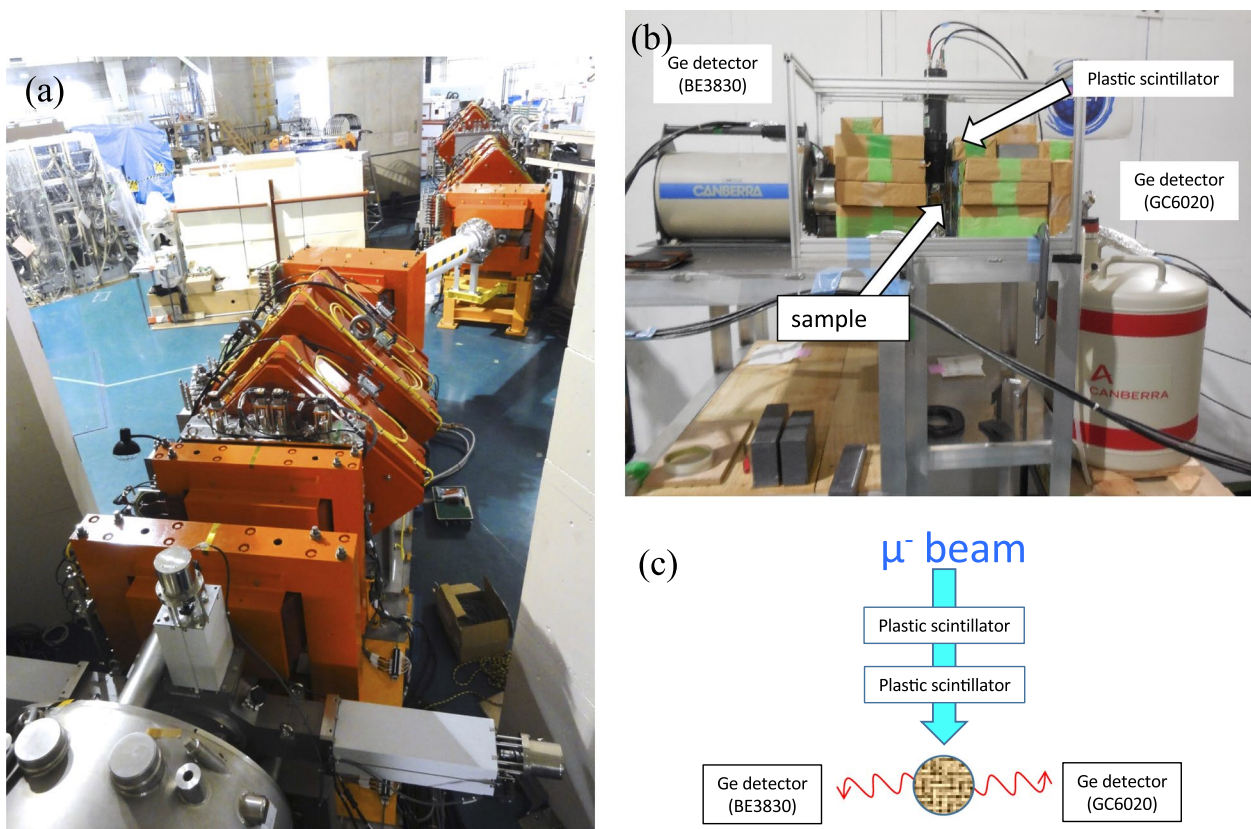


Fig. 2 **a** An entire view of the MuSIC (Muon Science Innovative Channel) beamline at RCNP (Research Centre for Nuclear Physics), Osaka University. **b** Outlet of the muon beam at the MuSIC. **c** A schematic illustration of an analytical setting

the muon beam were 2.0 h for the enriched ^{208}Pb sample and 6.4 h for the natural PbS, respectively.

Results and discussion

Figure 3a, b shows the muonic X-ray spectra obtained from an enriched ^{208}Pb sample and the natural galena (PbS) using the Ge-detector GC6020. Various muonic X-rays of Pb, such as Pb_{2-1} , Pb_{3-2} , Pb_{5-3} , Pb_{4-3} and Pb_{5-4} are detected due to a muon cascade process. On the other hand, the S_{2-1} peak at 516 keV appears only in the energy spectra of PbS (Fig. 3c). Other sulphur peaks are not shown because the energy of their muonic X-rays are too low (for example, 100 keV for S_{4-2} and/or 133 keV for S_{3-2}) in this experimental setting. Some gamma rays from the decay of thallium (Tl), which was a by-product of the muon nuclear capture such as $^{208}\text{Pb} (\mu^-, 0n) ^{208}\text{Tl}$, were also detected. The details of gamma rays from the decay of thallium (Tl) were discussed in Kudo et al. (2019).

Figure 4a shows an enlarged view of the muonic Pb_{2-1} X-ray spectra ($K_{\alpha 1(2p_{3/2-1s_{1/2})}$ and $K_{\alpha 2(2p_{1/2-1s_{1/2})}$) obtained by the Ge-detector GC6020. The enriched ^{208}Pb sample shows a sharp peak, whereas the natural galena (PbS) has broad peaks with a tail on the high-energy side. It is

noted that the low-energy component of the spread peak was consistent with the peak of the enriched ^{208}Pb sample and that the higher energy of the spread peak was consistent with the expected energy of the muonic X-ray of ^{207}Pb , ^{206}Pb and ^{204}Pb (Kessler et al. 1975).

Because the muon capture probability for each lead isotope is the same, that is, the sensitivity of each isotope is identical, the intensity ratio of muonic X-rays from ^{208}Pb , ^{207}Pb , ^{206}Pb and ^{204}Pb must be consistent with the isotopic composition. In order to derive the Pb isotopic composition, we carried out the deconvolution of the broad peaks by four muon-induced characteristic X-ray peaks as follows. First, the single peaks of the $K_{\alpha 1(2p_{3/2-1s_{1/2})}$ and $K_{\alpha 2(2p_{1/2-1s_{1/2})}$ X-rays of the enriched ^{208}Pb sample were fitted with a single Gaussian function, determining the peak centre and peak width. Then, the broad $K\alpha$ X-rays peaks of the natural galena (PbS) were fitted with four Gaussians functions for ^{208}Pb , ^{207}Pb , ^{206}Pb and ^{204}Pb with fixed the peak width, where the peak centres of ^{207}Pb , ^{206}Pb and ^{204}Pb were also assumed to be the literature values (Kessler et al. 1975). The obtained isotope ratios of Pb of the natural galena from the two X-ray peaks of two detectors are summarized in Tables 1 and

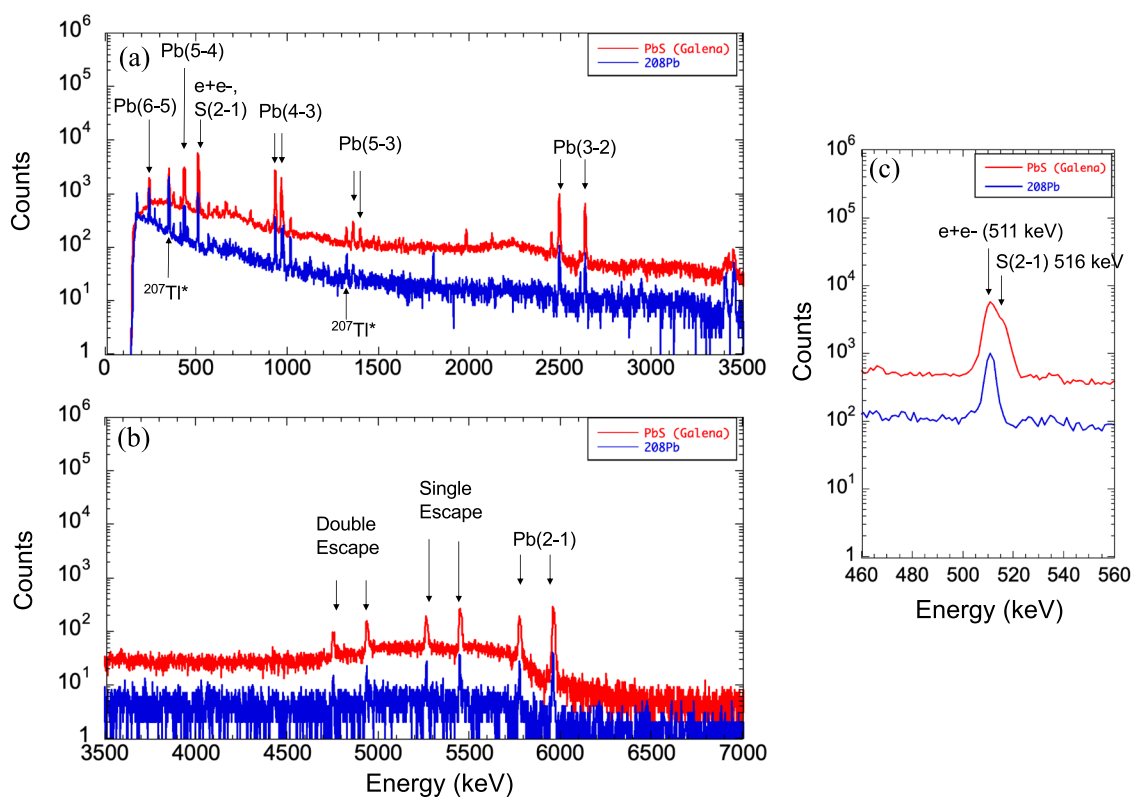


Fig. 3 **a, b** Whole muonic X-ray spectra of an enriched ^{208}Pb sample and the natural galena (PbS) obtained by Ge-detector GC6020. Cascading muonic Pb X-rays such as Pb_{2-1} , Pb_{3-2} , Pb_{5-3} , Pb_{4-3} and Pb_{5-4} lines were clearly observed. **c** Enlarged X-ray spectrum around 510 keV. Due to the S_{2-1} X-rays (516 keV), it can be observed that the peak width of PbS is broadened in comparison with that of the enrich ^{208}Pb sample

2, respectively. As shown in Fig. 5, the four-averaged isotope ratios obtained from the muonic Pb characteristic X-ray are in close agreement with those determined by the LA-ICP mass spectrometer within one sigma level. Thus, this study has demonstrated for the first time that the DC muon beam analysis is feasible for non-destructive isotope measurement of heavy elements in the natural samples, although the accuracy and precision are still insufficient for conducting the latest research in the research field of Earth and planetary science and archaeology (Table 3).

Finally, we emphasize that the isotopic shift in the energy of the muon-induced characteristic X-rays occurs for all isotopes (Wu and Wilets 1969; Engfer et al. 1974). This means that with further development of detectors, isotopic measurements of all natural samples (not only solid samples but also liquids and gases) can be taken non-destructively. Recently, advanced spectroscopy utilizing a transition edge sensor (TES) has been developed for harder X-ray spectroscopy (Guruswamy et al. 2018; Tatsuno et al. 2016; Okada

et al. 2016). Great advantages of TESs are to provide an order of magnitude better energy resolution than semiconductor-based detectors (for instance, the achieved energy resolution is 5.2 eV FWHM at Co K_{α} (6.9 keV) by Tatsuno et al. (2016) and 22 eV at 97.43 keV by Bacrania et al. (2009). That means TESs and/or cryogenic microcalorimeter have a great potential to distinguish the muonic K_{α} peak for lighter elements such as C (75.26 keV for ^{12}C and 75.31 keV for ^{13}C) and O (133.544 keV for ^{16}O and 133.572 keV for ^{18}O), and determine the isotope ratios not only heavy elements but also lighter elements without any destructive analysis. MuSIC facility also plans to increase the beam intensity by 15 times by reconstruction of the AVF cyclotron accelerator, which would improve the counting statistics problem. Thus, interdisciplinary further development such as higher-intensity DC muon beams and higher-energy-resolution detectors for hard X-rays would bring new “eyes” to see through the isotopic composition of planetary materials and/or archaeology artefacts non-destructively.

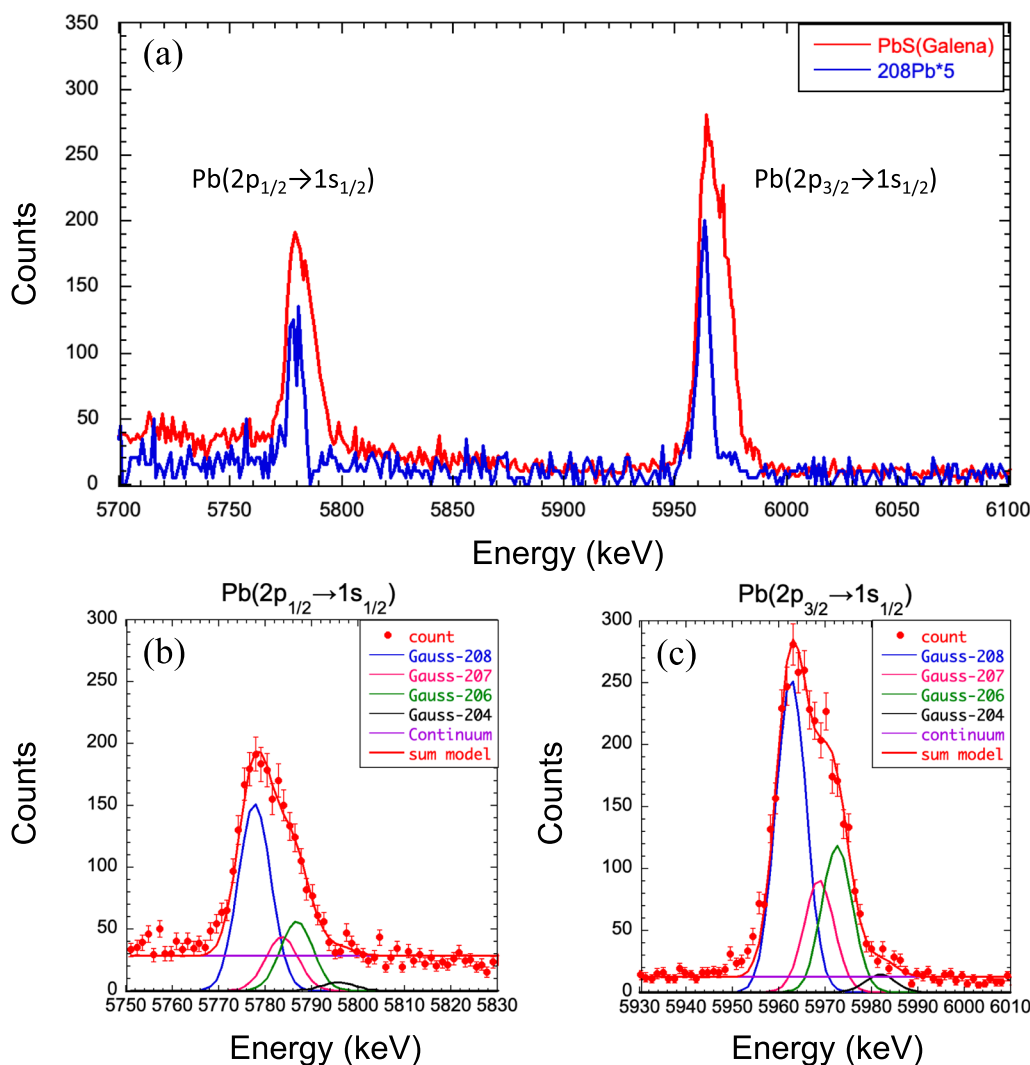


Fig. 4 **a** Enlarged view of the muonic Pb_{2-1} X-ray region. Due to the large energy splitting between muonic $2p_{1/2}$ and $2p_{3/2}$ states, $K_{\alpha 1(2p_{3/2} \rightarrow 1s_{1/2})}$ and $K_{\alpha 2(2p_{1/2} \rightarrow 1s_{1/2})}$ X-rays appear in two different energy regions. Each peak was a single sharp component in the enriched ^{208}Pb sample (blue line); on the other hand, it was broadening due to the presence of the lighter isotope of Pb in the PbS sample (red line). **b, c** Expanded spectrum of muonic $K_{\alpha 1}$ X-ray and $K_{\alpha 2}$ X-ray of Pb with the fitting component by four Gaussian functions with fixed peak width for ^{208}Pb , ^{207}Pb , ^{206}Pb and ^{204}Pb , where the peak centres of ^{206}Pb , ^{207}Pb and ^{204}Pb were also assumed to be the literature values (Kessler et al. 1975)

Table 1 Observed peak area and Pb isotope ratios from transition of $2p_{1/2} \rightarrow 1s_{1/2}$

	Energy (keV) ^a	Ge-detector BE3830		Ge-detector GC6020	
		Peak area	$^{xxx}Pb/^{208}Pb$	Peak area	$^{xxx}Pb/^{208}Pb$
Pb-208	5777.91 ± 0.40	737 ± 80	1.000 ± 0.108	1087 ± 146	1.000 ± 0.134
Pb-207	5783.79 ± 0.44	249 ± 62	0.338 ± 0.092	314 ± 104	0.289 ± 0.103
Pb-206	5787.00 ± 0.41	375 ± 60	0.509 ± 0.098	403 ± 96	0.370 ± 0.101
Pb-204	5796.06 ± 0.41	81 ± 34	0.110 ± 0.047	49 ± 48	0.045 ± 0.045
	Reduced Chi-square	0.90		1.42	
	Degrees of freedom	55		58	

^a Kessler et al. (1975)

Table 2 Observed peak area and Pb isotope ratios from transition of 2p3/2 → 1s1/2

	Energy (keV) ^a	Ge-detector BE3830		Ge-detector GC6020	
		Peak area	^{xxx} Pb/ ²⁰⁸ Pb	Peak area	^{xxx} Pb/ ²⁰⁸ Pb
Pb-208	5962.77 ± 0.42	1108 ± 61	1.000 ± 0.055	1710 ± 127	1.000 ± 0.074
Pb-207	5968.89 ± 0.44	428 ± 53	0.386 ± 0.052	611 ± 104	0.357 ± 0.066
Pb-206	5972.80 ± 0.41	665 ± 49	0.601 ± 0.055	799 ± 94	0.467 ± 0.065
Pb-204	5982.12 ± 0.41	102 ± 26	0.092 ± 0.024	95 ± 42	0.056 ± 0.025
	Reduced Chi-square	0.97		1.49	
	Degrees of freedom	55		55	

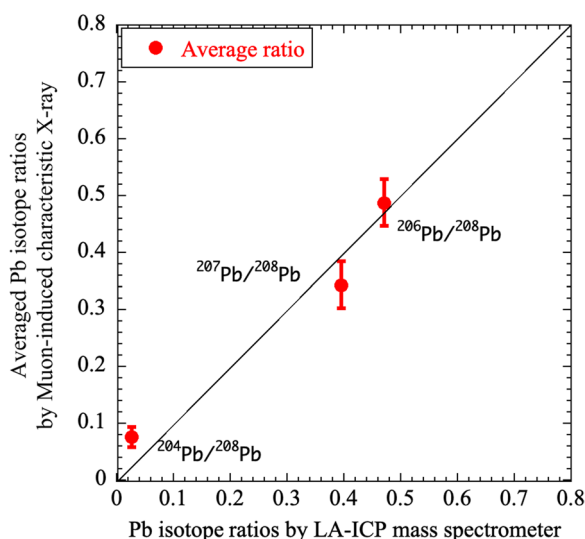


Fig. 5 Comparison with the four-averaged isotope ratios obtained from muonic characteristic X-ray with those determined by the LA-ICP mass spectrometer of the natural PbS (galena). Error bars are one sigma level

Table 3 Comparison of Pb isotope ratios of PbS obtained by muon analysis and LA-ICP mass spectrometer

	Average of muon analysis	LA-ICP mass
²⁰⁷ Pb/ ²⁰⁸ Pb	0.343 ± 0.040	0.396 ± 0.005
²⁰⁶ Pb/ ²⁰⁸ Pb	0.487 ± 0.041	0.472 ± 0.007
²⁰⁴ Pb/ ²⁰⁸ Pb	0.076 ± 0.018	0.026 ± 0.004

Acknowledgements

We appreciate Dr. Y. Hayasaka and Dr. K. Hoshino (Hiroshima University) for the LA-ICP mass spectrometer analysis. We thank all the staff of MuSIC and/or RCNP Cyclotron Facility. We are also grateful to the anonymous reviewer and the editor (Dr. Yuri Amelin) for instructive criticisms. The muon experiment at the MuSIC was performed under the RCNP cyclotron accelerator Beam-time Program (proposal no. E479 (48 hours) and E490 (12 hours)).

Author contributions

KT designed the research. KT and KN wrote the manuscript. AS, KN, DT, YK, MI, AN, TK, TO and MKK conducted the experiments. All authors contributed to the interpretation of the results and have read and approved the final manuscript.

Funding

This work was partly supported by Japan Society for the Promotion of Science KAKENHI Grants (17K18805, 18H03739 and 18K11922).

Availability of data and materials

All data generated or analysed during this study are included in this published article.

Declarations

Competing interests

The authors declare that they have no competing interests.

Received: 12 November 2023 Accepted: 11 April 2024

Published online: 07 May 2024

References

Bacrania MK, et al. Large-area microcalorimeter detectors for ultra-high-resolution X-ray and gamma-ray spectroscopy. *IEEE Trans Nucl Sci.* 2009;56:2299–302.

Chiu I-H, Terada K, Osawa T, Park C, Takeshita S, Miyake Y, Ninomiya K. Non-destructive elemental analysis of lunar materials with negative muon beam at J-PARC. *J Phys Conf Ser.* 2023;2462: 012004.

Cook S, et al. Delivering the world’s most intense muon beam. *Phys Rev Accel Beams.* 2017;20:030101.

Engfer R, et al. Charge-distribution parameters, isotope shifts, isomer shifts, and magnetic hyperfine constants from muonic atoms. *At Data Nucl Data Tables.* 1974;14:509–97.

Guruswamy T, Gades LM, Miceli A, Patel UM, Weizeorick JT, Quaranta O. Hard X-ray fluorescence measurements with TESs at the Advanced Photon Source. *J Phys Conf Ser.* 2018;1559:01.

Hino Y, et al. A highly intense DC muon source, MuSIC and muon CLFV search. *Nucl Phys B (proc Suppl).* 2014;253–255:206–7.

Jenkins DA, Powers RJ, Kunselman AR. Muonic Interactions in Zn⁶⁶ and Zn⁶⁸. *Phys Rev C.* 1970;2:458–61.

Kessler D, et al. Muonic X rays in lead isotopes. *Phys Rev C.* 1975;11:1719–34.

Kohno Y. Development on beam profile monitor for High-Intensity Muon source, MuSIC, Master thesis of Osaka University;2015 (in Japanese).

Kudo T, Ninomiya K, Strasser P, Terada K, Yosuke KY, Tampo M, Miyake Y, Shinohara A, Kubo KM. Development of a non-destructive isotopic analysis method by gamma-ray emission measurement after negative muon irradiation. *J Radioanal Nucl Chem.* 2019;322:1299–303.

Kunold W, Schneider M, Simons LM. Isotope shift measurements of muonic X-rays in 134,136,138Barium. *Z Phys A at Nucl.* 1983;312:11–7.

- Macagno ER, et al. Muonic atoms. II. Isotope shifts. *Phys Rev C*. 1970;4:1202–21.
- Miyake Y, et al. Birth of an intense pulsed muon source, J-PARC MUSE J-PARC muon source, MUSE. *Nucl Inst Methods Phys Res A*. 2009;600:22–4.
- Nakamura T, et al. Formation and evolution of carbonaceous asteroid Ryugu: direct evidence from returned samples. *Science*. 2022;379:eabn8671.
- Ninomiya K, et al. Non-destructive composition identification for mixtures of iron compounds using a chemical environmental effect on a muon capture process. *Bull Chem Soc Jpn*. 2022;95:1769–74.
- Ninomiya K, et al. Quantification of bulk elemental composition for C-type asteroid Ryugu samples by non-destructive elemental analysis method using muon beam. *Meteorit Planet Sci*. 2024. <https://doi.org/10.1111/maps.14135>.
- Ninomiya K, Kudo T, Strasser P, Terada K, Kawai Y, Tampo M, Miyake Y, Shinohara A, Kubo MK. Development of non-destructive isotopic analysis methods using muon beams and their application to the analysis of lead. *J Radioanal Nucl Chem*. 2019;320:801–5.
- Okada S, et al. First application of superconducting transition-edge sensor microcalorimeters to hadronic atom X-ray spectroscopy. *Progress Theor Exp Phys*. 2016;9:091D01.
- Osawa T, et al. Isotopic ratio analysis using muon X-ray. *KEK Progress Report*. 2020;2020–4:64–5.
- Osawa T, Ninomiya K, Yoshida G, Inagaki M, Kubo MK, Kawamura N, Miyake Y. Elemental analysis system with negative-muon beam. *JPS Conf Proc*. 2015;8:025003(1-6).
- Osawa T, Nagasawa S, Ninomiya K, Takahashi T, Nakamura T, Wada T, Taniguchi A, Umegaki I, Kubo M, Terada K, Chiu I-H, Takeda S, Katsuragawa M, Minami T, Watanabe S, Azuma T, Mizumoto K, Yoshida G, Takeshita S, Tampo M, Shimomura K, Miyake Y. Development of non-destructive elemental analysis system for Hayabusa2 samples using muonic X-rays. *ACS Earth Space Chem*. 2023;4:699–711.
- Schellenberg L. Systematics of nuclear charge radii of the stable molybdenum isotopes from muonic atoms. *Nucl Phys A*. 1984;333:333–42.
- Shera R, et al. Nuclear charge radii of the Te isotopes from muonic atoms. *Phys Rev C*. 1989;39:135–208.
- Strasser P, et al. Muon spectroscopy with trace alkaline-earth and rare-earth isotopes implanted in solid D2. *Hyperfine Interact*. 2009;193:121–7.
- Tatsuno H, et al. Absolute energy calibration of X-ray TESs with 0.04 eV uncertainty at 6.4 keV in a hadron-beam environment. *J Low Temp Phys*. 2016;184:930–7.
- Terada K, et al. A new X-ray fluorescence spectroscopy for extraterrestrial materials using a muon beam. *Sci Rep*. 2014;4:5072.
- Terada K, et al. Non-destructive elemental analysis of a carbonaceous chondrite with direct current Muon beam at MuSIC. *Sci Rep*. 2017;7:15478. Virginia Polytechnic Institute, Blacksburg, Virginia 24061
- Wu CS, Wilers L. Muonic atoms and nuclear structure. *Annu Rev Nuclear Sci*. 1969;19:527–606.

Publisher's Note

Springer Nature remains neutral with regard to jurisdictional claims in published maps and institutional affiliations.